Volume 11
Number 35
21 September 2020
Pages 9327–9716

Chemical Science

rsc.li/chemical-science

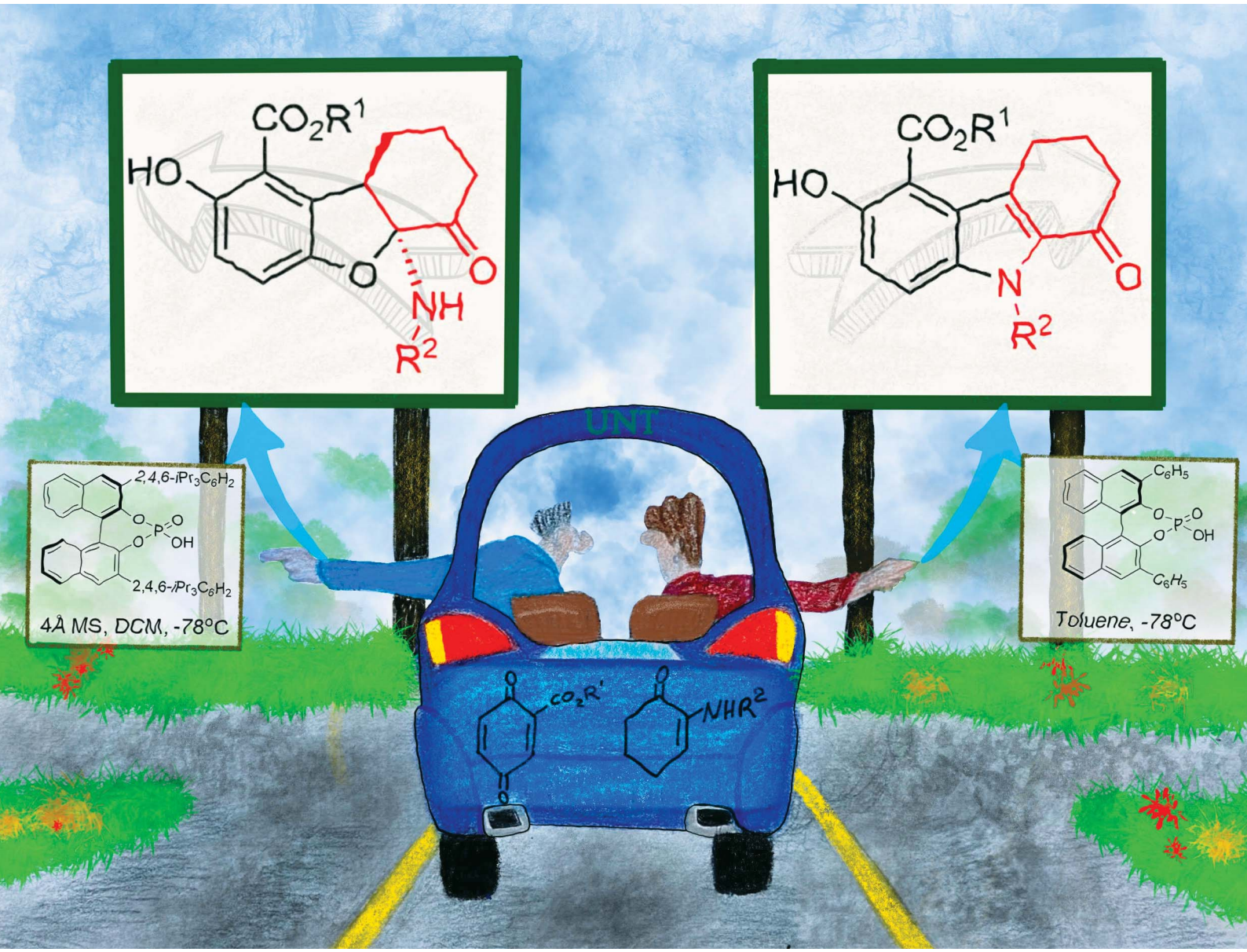

ISSN 2041-6539

ROYAL SOCIETY OF CHEMISTRY

EDGE ARTICLE

Thomas R. Cundari, Hong Wang *et al.*

Formal oxo- and aza-[3 + 2] reactions of α-enaminones and quinones: a double divergent process and the roles of chiral phosphoric acid and molecular sieves

Chemical Science

ROYAL SOCIETY OF CHEMISTRY

EDGE ARTICLE

View Article Online
View Journal | View Issue

Cite this: *Chem. Sci.*, 2020, **11**, 9386

All publication charges for this article have been paid for by the Royal Society of Chemistry

Formal oxo- and aza-[3 + 2] reactions of α-enaminones and quinones: a double divergent process and the roles of chiral phosphoric acid and molecular sieves†

Weiwei Luo, Zhicheng Sun, E. H. Nisala Fernando, Vladimir N. Nesterov, Thomas R. Cundari* and Hong Wang *

Received 12th April 2020
Accepted 7th July 2020

DOI: 10.1039/d0sc02078h

rsc.li/chemical-science

A double divergent process has been developed for the reaction of α-enaminones with quinones through facile manipulation of catalyst and additive, leading to structurally completely different products. The two divergent processes, which involve formal aza- and oxo-[3 + 2] cycloaddition reactions, are mediated by chiral phosphoric acid and molecular sieves, respectively. While inclusion of phosphoric acid in the reaction switched the reaction pathway to favor the efficient formation of a wide range of *N*-substituted indoles, addition of 4 Å molecular sieves to the reaction switched the reaction pathway again, leading to enantioselective synthesis of 2,3-dihydrobenzofurans in excellent yields and enantioselectivities under mild conditions. Studies in this work suggest that the chiral phosphoric acid acts to lower the transition state energy and promote the formation of amide intermediate for the formal aza-[3 + 2] cycloaddition and the molecular sieves serve to facilitate proton transfer for oxo-[3 + 2] cycloaddition. The reactivity of α-enaminones is also disclosed in this work.

Introduction

Divergent reactivity is an effective tool to control product distribution, and has remained an intense research interest in chemical catalysis, synthetic organic chemistry and pharmaceutical sciences.[1,2] Despite the challenges in developing divergent reactions, a growing number of switchable organic transformations have been achieved through divergent reactions in the past decade. The predominant strategy to access divergent reactions is to develop different catalysts to attain product selectivity *via* different catalytic intermediates (catalyst-controlled selectivity) (Scheme 1a). On the other hand, using the same catalyst to access structurally different compounds from the same reactants (additive-controlled) is extremely challenging,[2a,b,p] as the divergent reactions are expected to share the same catalytic intermediates. In an early work, Jørgensen and co-workers designed an additive-controlled divergent synthesis of tetrahydrothiophenes (Scheme 1b).[2a] This divergent reaction utilized the same proline catalyst and shared the same key intermediate (**X**). Treatment of the key intermediate (**X**) with different additives, *i.e.*, PhCOOH and $NaHCO_3$, respectively, leads to tetrahydrothiophenes with different substitution

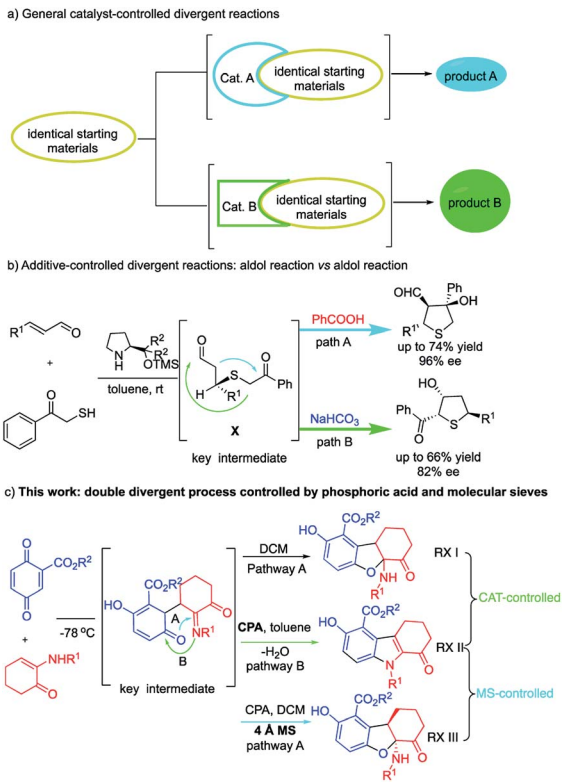

Scheme 1 Catalytic divergent transformations.

Department of Chemistry, University of North Texas, Denton, TX 76203, USA. E-mail: thomas.cundari@unt.edu; hong.wang@unt.edu

† Electronic supplementary information (ESI) available. CCDC 1919282, 1921254 and 1919286. For ESI and crystallographic data in CIF or other electronic format see DOI: 10.1039/d0sc02078h

patterns through competitive aldol pathways. Jørgensen's work suggested the possibility for additive-controlled divergent reactions.

In the present work, we reveal a rare double divergent process, which was mediated by phosphoric acid (catalyst-controlled) and molecular sieves (additive-controlled), respectively. α-Enaminone reacting with quinone in the absence of a catalyst or an additive afforded 2,3-dihydrobenzofurans (Scheme 1c, **RX I**). Upon addition of chiral phosphoric acid, the reaction pathway switched to forming *N*-substituted indoles (Scheme 1c, **RX II**). When molecular sieves were included in the reaction, the reaction pathway switched back to form enantioenriched tricyclic 2,3-dihydrobenzofurans (**RX III**). Thus, two divergent processes were realized. The first divergent process was controlled by phosphoric acid, and the second divergent process was controlled by molecular sieves (M.S.). This work represents, to our knowledge, the first example of a double divergent process. It is also the first example of molecular sieve-controlled divergent reaction. The functions of the phosphoric acid and the molecular sieves were investigated both experimentally and theoretically, and a new role of molecular sieves has been unveiled. This work provides concise new approaches to access important 2,3-dihydrobenzofurans and indoles, both of which are widespread structural skeletons found in biomolecules, natural products, pharmaceuticals, and have attracted significant research endeavors.[3]

Enaminones are important synthetic intermediates in organic synthesis.[4,5] Enaminones including α-enaminones and β-enaminones (Fig. 1) often display multi-functionality, as they possess both nucleophilic (enamine) and electrophilic (enone) characteristics. Unlike β-enaminones, which have been frequently used in the synthesis of natural products and other biological active compounds,[4] little attention has been paid to α-enaminones due to the lack of appropriate synthetic routes of their synthesis.[5] We became interested in α-enaminones during our investigation in cooperative enamine-metal Lewis acid catalysis.[6] It was found that α-enaminones could be readily formed from arylamine and cyclohexanone in the presence of a metal Lewis acid under ambient conditions.[5e] This discovery prompted us to investigate the reactivities of α-enaminones as they remain largely unexplored. It is expected that α-enaminones will display different set of reactivities from β-enaminones, as β-enaminones are linearly conjugated molecules and α-enaminones are cross-conjugated molecules. In this work, we demonstrate that α-enaminones display multifunctionality, acting as both an enamine and a nitrogen nucleophile, as well as an imine electrophile to initiate two novel phosphoric acid-catalyzed [3 + 2] cycloaddition reactions through 1,4-ketone/imine intermediate (Paal–Knorr type intermediates).[7]

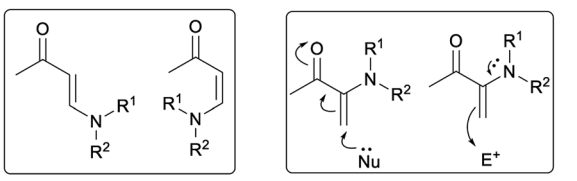

Fig. 1 α- and β-enaminones.

Results and discussion

Quinone ester was selected as the reaction partner for α-enaminone due to its high activity and multifunctionality.[8] Quinone ester **1a** reacted smoothly with enaminone **2a** without any catalyst, affording a formal oxo-[3 + 2] product **3a** in 85% yield (Table 1, entry 1). While it was exciting that an interesting new reaction was discovered, this strong background reaction makes it challenging to develop an asymmetric version of this reaction.

Considering the possible mechanism and multiple functional groups capable of H-bonding present in the substrates, a chiral phosphoric acid (**CPA1**) was chosen to mediate this reaction. Surprisingly, a new product was obtained in 90% yield along with **3a** in 10% yield and 18% ee (entry 2). This new product turned out to be a *N*-substituted indole (**4a**) formed *via* a formal aza-[3 + 2] cycloaddition. These data suggest: (1) phosphoric acid can catalyze this reaction, initiating a divergent process; (2) chiral phosphoric acid could induce ee of **3a**. A series of chiral phosphoric acid catalysts were then tested (Table 1, entries 3–6). Increasing the steric bulk (from H, Me, to Ph) at the 3,3′-position of the **CPA** resulted in increased yield and ee of **3a** at the cost of **4a** (entries 2–4). Based on these data, it

Table 1 Condition screening and optimization[a]

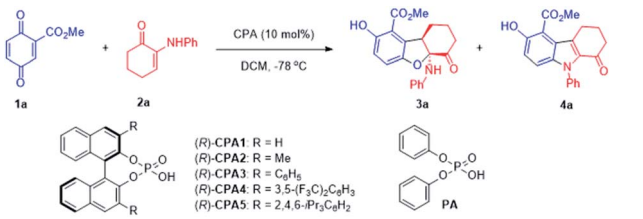

Entry	Cat.	Yield[b] (%) 3a	4a	ee of 3a[c] (%)
1	—	85	—	0
2	**CPA1**	10	90	18
3	**CPA2**	14	77	20
4	**CPA3**	34	63	90
5	**CPA4**	78	17	72
6	**CPA5**	16	78	99
7[d]	**CPA5**	97	—	99
8[d,e]	**CPA5**	98	—	99
9[f,g]	**CPA3**	—	96	—
10[f,g,h]	**CPA3**	—	99	—
11[g]	**PA**	8	84	—

[a] Unless otherwise noted, all reactions were carried out with **1a** (0.1 mmol), **2a** (0.11 mmol), **CPA** (10 mol%) in 1.0 mL DCM at −78 °C for 16 h. [b] Isolated yield. [c] Determined by chiral HPLC analysis. [d] 5.0 mg of 4 Å M.S. [e] 1.0 mol% of catalyst was used. [f] Toluene (1.0 mL) as solvent. [g] 0.1 mmol of **2a** was used. [h] 5.0 mol% of catalyst was used.

appeared that increasing the steric bulkiness of **CPA** slightly favors the formation of **3a** and results in higher ee of **3a**. When **CPA4** containing bulky 3,5-bis(trifluoromethyl)phenyl groups was used, the yield of **3a** increased to 78% but the ee decreased to 72% (entry 5). When a highly bulky group, *i.e.*, 2,4,6-tri(isopropyl)phenyl, was attached at the 3,3′-positions of **CPA** (entry 6), although the yield of **3a** decreased significantly with increased yield of **4a**, the ee of **3a** increased to 99%. These data suggest that a stronger acid is likely to facilitate the formation of **3a**, however, at the cost of enantioselectivity; on the other hand, increased steric bulkiness of **CPA** enhances the enantioselectivity of **3a**.

Inspired by Rueping's[9a] and Wang's reviews[9b] on phosphoric acids and additive effects, in which M.S. could promote some organic transformations catalyzed by phosphoric acid, M.S. were then attempted to mediate the **3a** forming reaction. It was a surprise that addition of 4 Å M.S. completely switched the reaction pathway of the **CPA5** catalyzed reaction (entry 7) to favor **3a** formation. While the yield of **3a** increased to 97%, the enantioselectivity of **3a** remained at 99%. It is notable that decreasing **CPA5** loading to 1 mol% led to comparable results (entry 8, 98% yield, 99% ee). These data suggest that molecule sieves initiated another divergent process.

To optimize the reaction condition for **4a**, solvent was surveyed. In the presence of **CPA** without M.S., reactions in most of the solvents favored the formation of **4a**. Toluene appeared to be the best to promote **4a** (entries 9–11, 92–96% yields). Decreasing **CPA3** loading from 10% to 5 mol% has no negative effect (entry 10, 99% yield). Considering that the employment of a chiral phosphoric acid to produce achiral products is not cost-effective, we examined an achiral phosphoric acid as the catalyst. Diphenyl phosphate (**PA**) turned out to be suitable for such reaction, and the desired product **4a** was obtained in 84% yield (entry 11).

Having a controllable new synthesis in hand, the substrate scope for both reactions were investigated. The substrate scope of 2,3-dihydrobenzofuran synthesis is broad (Table 2). Various quinones and α-enaminones reacted smoothly to afford tricyclic 2,3-dihydrobenzofurans (**3a–3x**) in good yields (39–99%) with excellent diastereoselectivities (91 : 9 → 95 : 5 d.r.) and enantioselectivities (95–99% ee). Changing the ester (R^1) group of quinone from methyl to ethyl and benzyl didn't affect the reactivity and enantioselectivity (**3a–c**). Regarding the *ortho* substituents on the phenyl ring of α-enaminones, a weak electron-donating group such as methyl (**3d**) gave slightly better yield (96%) than slightly electron-withdrawing groups such as chlorine and bromine (**3e** & **3f**, 85% and 81% respectively), while the stereoselectivity of these substrates were similar. Substituents at the *meta* and *para* position are equally well tolerated. Both electron-donating and electron-withdrawing groups provided the corresponding products in high yields and enantioselectivities (**3g–s**). Multisubstituted and naphthalenyl-substituted α-enaminones also proceeded smoothly to give the corresponding products in up to 99% yield with excellent stereoselectivity (**3t–v**). α-Enaminone derived from cyclopentanone was also investigated. While the enantioselectivity remained high (**3w**, 99% ee), the yield decreased to 39% likely due to ring strain. Enaminone derived from substituted cyclohexanone generated product **3x** in good yield of the major diastereomer with excellent enantioselectivity. The absolute configuration of **3a** was established unambiguously to be (5a*S*,9a*R*) through X-ray crystallographic analysis (Table 2, CCDC 1919282).[10]

α-Enaminones derived from an aliphatic amine, *i.e.*, benzylamine, did not give the expected 2,3-dihydrobenzofuran derivative (**3y**). Instead, 2,3-dihydrobenzofuran bearing a hydroxy group (**3z**) was obtained in 92% yield and 92% ee (Scheme 2, eqn (1)). The structure and the absolute configuration of **3z** was assigned to be (5a*S*,9a*R*) with X-ray crystallographic analysis (CCDC 1921254).[10] Theoretically, product **3z** could result from the hydrolysis of **3y** (Scheme 2, eqn (1)). It is

Table 2 Enantioselective synthesis of tricyclic 2,3-dihydrobenzofurans[a,b,c]

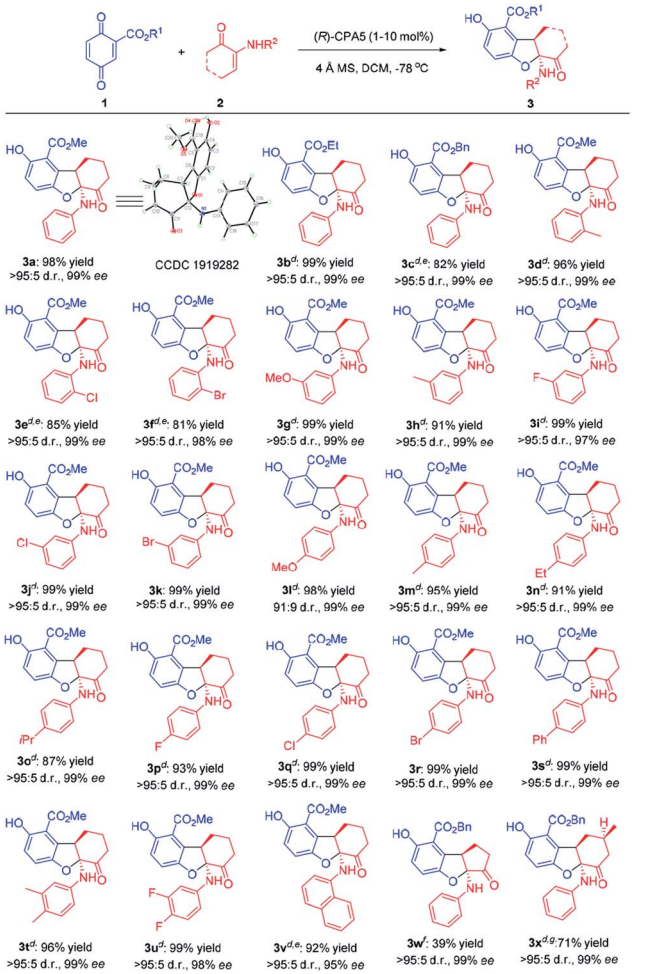

[a] All reactions were carried out with **1** (0.1 mmol), **2** (0.11 mmol), 4 Å M.S. (5.0 mg) and (*R*)-**CPA5** (1.0 mol%) in CH_2Cl_2 (1.0 mL) at −78 °C for 16 h. [b] Isolated yield. [c] The d.r. and ee values of the products were determined by HPLC analysis on a chiral stationary phase. [d] 20.0 mg of 4 Å M.S. [e] 5.0 mol% of (*R*)-**CPA5**. [f] The reaction was conducted on 0.05 mmol scale with 10 mol% of (*R*)-**CPA5** and 10.0 mg of 4 Å M.S. at −60 °C. [g] **2w** (0.22 mmol) and (*R*)-**CPA5** (10.0 mol%) at −60 °C, isolated yield of the major diastereomer.

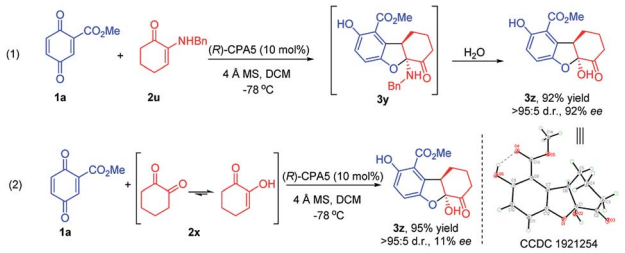

Scheme 2 Catalytic formation of 2,3-dihydrobenzofuran **3w**.

also possible that **2u** first decomposes to 1,2-cyclohexanedione **2x**, then react with **1a** producing **3z**. Reaction of **1a** with **2x** generated **3z** in high yield (95%), however, the ee was low (11%) (Scheme 2, eqn (2)). These data suggest that **3z** obtained from enaminone **2u** was through hydrolysis of intermediate **3y**, and that the activity of aliphatic amine derived enaminones is different from arylamine derived enaminones.

To probe the interactions between **CPA** with α-enaminone **2u** and 1,2-cyclohexanedione **2x**, control ^{1}H NMR experiments were carried out. Analysis of these ^{1}H NMR spectra (Fig. S5 and S6, see ESI†) suggests that the interaction between **CPA5** and α-enaminone **2u** is significantly stronger than that of **CPA** and **2x**, supporting the reaction pathway hypothesized above. These data also further support our earlier hypothesis that chiral phosphoric acid could mediate this reaction due to the existence of multifunctional groups capable of H-bonding in the starting materials.

Next, the substrate scope for *N*-substituted indoles was screened (Table 3). Quinone **1a** reacted with α-enaminone **2a** to afford **4a** in 99% yield. When the ester group of quinone **1** changed from methyl to ethyl and benzyl, the yields were somewhat decreased (**4b** & **4c**). α-Enaminones, which bear both electron-donating and electron-withdrawing substituents at the *para*-position of the phenyl ring gave high yields of indoles (**4i–4p**). α-Enaminones carrying electron-donating substitutes at the *meta*-position of the phenyl ring resulted in higher yields than α-enaminones carrying electron-withdrawing substitutes at the *meta*-position. 3,4-Disubstitution on the phenyl ring of α-enaminones also led to the formation of indoles in good yields (**4q** & **4r**). This reaction turned out to be challenging for α-enaminones with *ortho* substituents on the phenyl ring, producing the desired indoles in only 10% yield (Table S1, see ESI†). Nevertheless, this method could potentially provide an easy access to indoles with axial chirality, which is a hot topic currently,[11] and is worthy of further investigation. *N*-Benzyl protected indoles (**4s**) was obtained in low yield (31%), once again demonstrating different activity of arylamine-based α-enaminones from aliphatic amine-based α-enaminones. Notably, α-enaminones derived from cyclopentanone and 4-methyl cyclohexanone generated adducts **4t** (40% yield) and **4u** (48% yield), respectively. It was noteworthy that condition B using an achiral phosphoric acid as the catalyst exhibited good yields with selected substrates. The structure of **4a** was confirmed with X-ray crystal analysis (Table 3, CCDC 1919286).[10]

Table 3 Synthesis of *N*-substituted indoles[a,b]

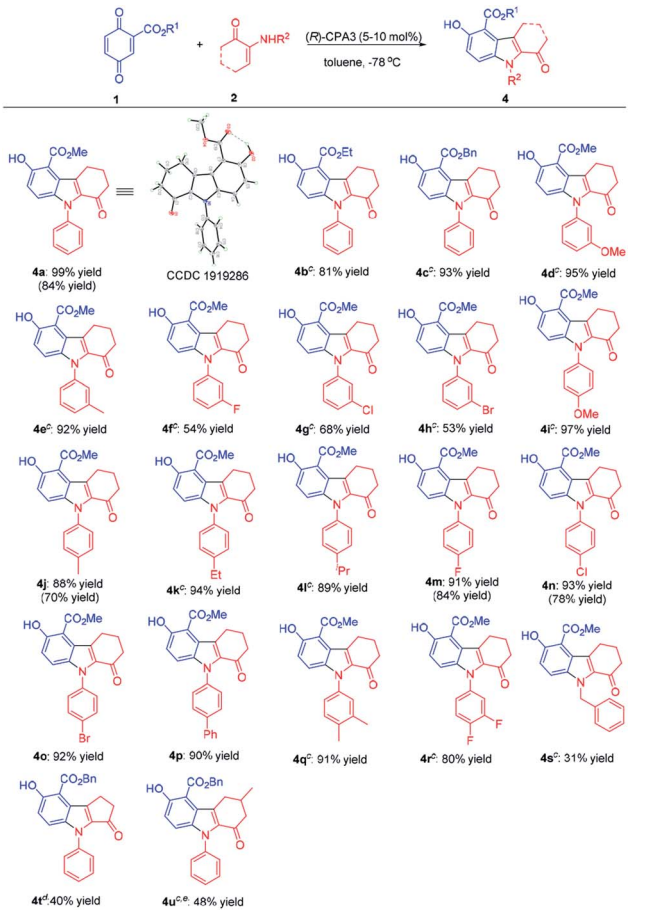

[a] Condition A: **1** (0.1 mmol), **2** (0.1 mmol) and (*R*)-**CPA3** (5.0 mol%) in toluene (1.0 mL) at −78 °C for 16 h; condition B: **1** (0.1 mmol), **2** (0.1 mmol) and **PA** (10 mol%) in DCM (1.0 mL) at −78 °C for 16 h. [b] Isolated yield of condition A, the results in parentheses were obtained with condition B. [c] 10 mol% of (*R*)-**CPA3**. [d] The reaction was conducted on 0.05 mmol scale with 10 mol% of (*R*)-**CPA5** at −60 °C. [e] At −60 °C for 18 h.

To show the prospect of the current methodologies in synthesis, the divergent reaction of quinone ester **1a** with α-enaminone **2a** was expanded to gram scale (3.0 mmol), and the desired 2,3-dihydrobenzofuran product **3a** was obtained in 94% yield with 98% ee (Scheme 3a). Reduction of the carbonyl group in **3a** using $NaBH_4$ afforded β-amino alcohol **5** in excellent yield with the retention of the enantioselectivity (Scheme 3b).

Control experiments were carried out to probe the roles of phosphoric acid and M.S. playing in this reaction (Table 4). The general function of M.S. is to take out water from a reaction. Molecule sieves are also known to mediate the interaction of water with substrates/intermediates in a reaction.[9b,12] Reactions with nonactivated 4 Å M.S. or freshly activated 4 Å M.S. (entries 1 and 2) gave similar results, both generating benzofuran **3a** as the major product in high enantioselectivity (99% ee). However, when dry $MgSO_4$ was used instead of M.S. (entry 9), the reaction pathway switched to favor the formation of **4a**, similar to the reaction without inclusion of M.S. (entry 3). When wet 4 Å M.S.

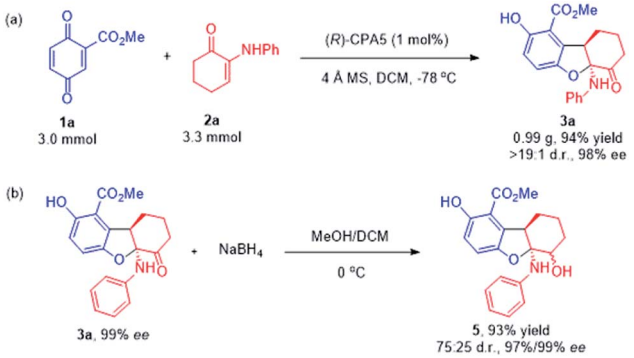

Scheme 3 (a) Gram-scale version of the reactions. (b) Synthetic utility.

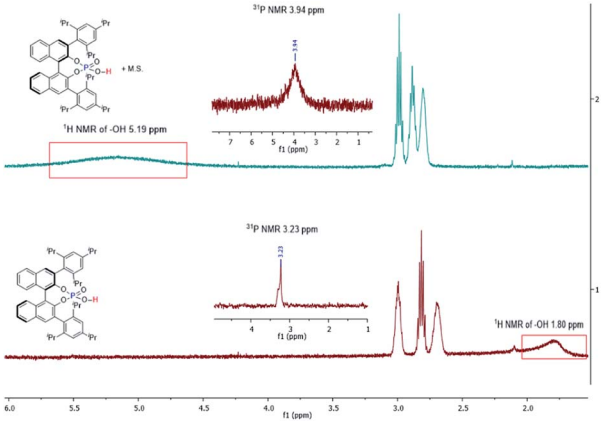

Fig. 2 ^{1}H and ^{31}P NMR spectra for the investigation of the interaction of phosphoric acid with M.S. in C_6D_6.

was used (entries 6 & 8), the formation of **3a** slowed down, at the same time the formation of **4a** sped up. These results suggest that, (1) M.S. is not serving a drying reagent for this reaction; (2) extra water added to this reaction influences the reaction pathways to slightly favor indole **4a** formation. It was noticed that the size and format of M.S. also affected the results of this reaction (entries 1, 4, 5, & 7). We suspect that the M.S. acts to facilitate proton (H^+) transfer.[9b] ^{1}H NMR and ^{31}P NMR spectroscopy of chiral phosphoric acid ((*R*)-**CPA5**) with and without M.S. were then conducted in benzene-d_6 (Fig. 2). In the absence of M.S., a broad peak was found for the phosphoric acid proton centered at 1.80 ppm; addition of M.S. broadened and shifted this peak significantly to the downfield centered at 5.19 ppm. Similar changes were observed on ^{31}P NMR spectra, with a phosphine peak at 3.23 ppm without M.S., and 3.94 ppm in the presence M.S. It is evident from these experiments that M.S. can potentially affect the acidity of phosphoric acid and mediate the interaction between a substrate and a catalyst.

In order to further illustrate the role of the phosphoric acid, an experiment with a different acid, *i.e.*, benzoic acid, was conducted (entry 10), leading to similar results with the background reaction (Table 1, entry 1). This result suggests that the strength of the acid matters in this reaction. Experiments with inclusion of a tertiary amine in the presence and absence of M.S. were also conducted (entries 11 & 12). Both reactions generated **3a** as the only product, however, with 0% ee, and in much decreased yields as compared with the background reaction. These data indicate: (1) the acid function of the phosphoric acid is important for this reaction, (2) M.S. is likely to mediate proton transfer in this reaction, as no effect of M.S. was observed after the phosphoric acid was neutralized with a tertiary amine.

Table 4 Mechanistic control experiments[a]

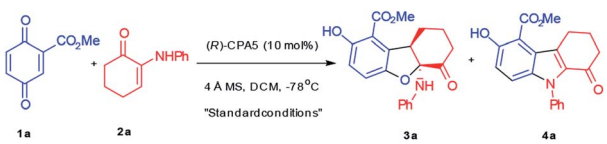

Entry	Variation from the "standard conditions"	Conv.[b] (%)	**3a** : **4a**[b]	ee of **3a**[c] (%)
1	None	97	>20 : 1	99
2	Freshly activated 4 Å M.S.	86	20 : 1	99
3	No M.S.	94	1 : 4.9	99
4	3 Å M.S. instead of 4 Å M.S.	95	>20 : 1	99
5	5 Å M.S. instead of 4 Å M.S.	94	11 : 1	99
6[d]	Wet 4 Å M.S.	99	1 : 1.1	99
7	4 Å M.S. (beads)	99	1 : 1	99
8[d]	Wet 4 Å M.S. (beads)	99	1 : 5.3	99
9	Dry $MgSO_4$ instead of 4 Å M.S.	99	1 : 4.2	99
10	Benzoic acid only	85	5 : 1	0
11[e]	Et_3N without 4 Å M.S.	15	>20 : 1	0
12	Et_3N with 4 Å M.S.	13	>20 : 1	0

[a] All reactions were carried out with **1a** (0.1 mmol), **2a** (0.11 mmol), 4 Å M.S. (5.0 mg) and (*R*)-**CPA5** (10 mol%) in CH_2Cl_2 (1.0 mL) at −78 °C for 16 h. [b] Determined by ^{1}H NMR. [c] Determined by HPLC analysis on a chiral stationary phase. [d] Freshly activated 4 Å M.S. and H_2O (2 μL). [e] M.S. and phosphoric acid were not present.

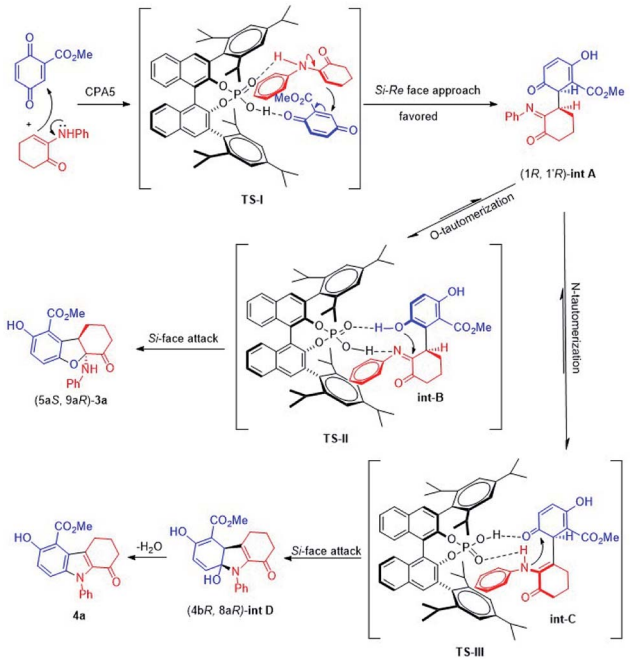

Scheme 4 Proposed mechanism.

A mechanism is proposed to illustrate the reaction process and stereocontrol of the divergent reaction based on the experimental data and X-ray structures of **3a** and **4a** (Scheme 4). α-Enaminone acts as an enamine nucleophile to attack from the *Si* face at the *Re* face of the quinone (Michael addition) through **TS-I** to form intermediate (1*R*,1′*R*)-**int A**. **TS-I**′ is expected to be disfavored due to steric hindrance (Fig. S12, see ESI†). Intermediate (1*R*,1′*R*)-**int A** equilibrates to intermediate **int B** and **int C** through *O*-tautomerization (enol/phenol from quinone) and *N*-tautomerization (enamine from imine), respectively. Intermediate **int B** and **int C** then bind **CPA** as illustrated in transition states **TS-II** and **TS-III**. **TS-II** leads to the formation of 2,3-dihydrobenzofuran ((5a*S*,9a*R*)-**3a**) through hydroxy group attack at the *Si* face of the imine, and **TS-III** gives rise to intermediate **int D** though amine group attack at the *Si* face of the carbonyl group followed by dehydroxylation to afford indole (**4a**). **TS-II** is more polarized in nature than **TS-III**, as imine nitrogen is a better proton acceptor than carbonyl oxygen, and hydroxy group in phenol is a better acid than amines. As such, in a more polar solvent such as DCM, **TS-II** is better stabilized. The addition of 4 Å molecular sieves (M.S.) is likely to facilitate the proton transfer in **TS-II** through absorbing/releasing proton.[9b] In non-polar solvent such as toluene, **TS-II** is destabilized, and the reaction through **TS-III** becomes dominant.

DFT calculations (B3LYP/6-311+G(d,p)/CPCM-DCM//B3LYP/6-31G(d)) are performed to gain more mechanistic insight into this novel double divergent process. The calculated free energy profile is shown in Fig. 3 to illustrate the reaction process and stereocontrol of the divergent reaction based on the experimental and computational data and X-ray structures of **3a** and **4a**. α-Enaminone and quinone ester coordination to the phosphoric acid forming the heterotrimer is used as the reference point for the free energy profile. Formation of the adduct (**B**) is shown to be 2 kcal mol^{-1} more favored in free energy than the separated reactants (**A**). To form intermediate **int A** (**D**), α-enaminone acts as an enamine nucleophile to attack the quinone (Michael addition) through **TS-I** with a barrier of 10.9 kcal mol^{-1}. The formation of **int A** intermediate coordination complex (**C**) is close to thermoneutral, which is 0.7 kcal mol^{-1} more stable than the reactant adducts (**B**). The

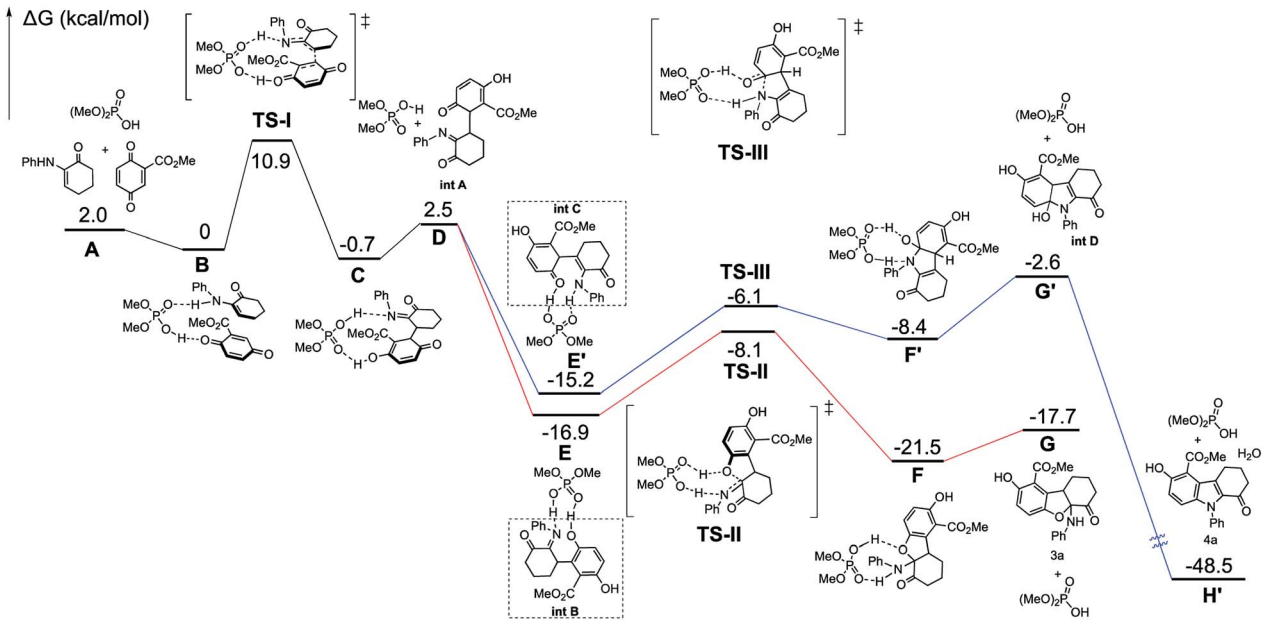

Fig. 3 Free-energy profiles calculated for the pathways catalyzed by phosphoric acid. The relative free-energies are in kcal mol^{-1}.

dissociation of **int A** and the rotation of C–C bond formed in **TS-I** is calculated to be 3.2 kcal mol^{-1} uphill from **C** to **D**. Intermediate **int A** equilibrates to intermediate **int B** and **int C** through *O*-tautomerization (enol/phenol from quinone) and *N*-tautomerization (enamine from imine), respectively. Calculations show that *O*-tautomerization and forming new hydrogen bonds with **CPA** (**E′**) is 15.2 kcal mol^{-1} downhill and that of *N*-tautomerization (**E**) is exergonic by 16.9 kcal mol^{-1} relative to reactant adduct **B**.

TS-II leads to the formation of 2,3-dihydrobenzofuran (**3a**) through hydroxy group attack of the imine. **TS-III** gives rise to intermediate **int D** though amide group attack the carbonyl group followed by dehydroxylation to afford indole (**4a**). The calculated barriers for **TS-II** and **TS-III** are 8.8 kcal mol^{-1} and 9.1 kcal mol^{-1}, respectively. We calculated different initial geometries of hydrogen-bonding modes for **TS-III** between the amide and the phosphoric acid. The optimized structure of **TS-III** suggests the proton transfer between the catalyst and **int C** and the amide dissociation from the catalyst happen prior to the amide attack. **TS-II** is more polarized in nature than **TS-III**, as amide nitrogen is a better proton acceptor than carbonyl oxygen, and hydroxy group in phenol is a better acid than amines.

Calculations on enantio-determining TSs with full **CPA5** catalyst shows that **TS-I′** is disfavored by 13.7 kcal mol^{-1} compared to **TS-I** (Fig. 4). No significant steric clashes were observed in the TS structures. But the structure of **TS-I** shows that the quinone ester is not coordinated to the catalyst, while **CPA5**, **1a** and **2a** form heterotrimer *via* hydrogen bonding with the catalyst in **TS-I′**. This result suggests that locking the two substrates is not necessary for lowering the activation barrier, especially if larger and more sterically shielding groups are used on the catalyst. Computational results also show that the formation of (1*R*,1′*R*)-**int A** is favored by 5.6 kcal mol^{-1} in free energy compared to (1*R*,1′*S*)-**int A**. The background reaction without catalyst is also calculated with the same level of theory (Fig. S15, see ESI†). **TS-I** has a much higher barrier without the catalyst (18.9 kcal mol^{-1}) than with catalyst (10.9 kcal mol^{-1}). Calculations show that **TS-II** is slightly stabilized (~1 kcal mol^{-1}) when catalyst is present. The reaction did not proceed *via* **TS-III** without catalyst is likely due to the inability to form amide for the attack without activation by phosphoric acid (Fig. 5).

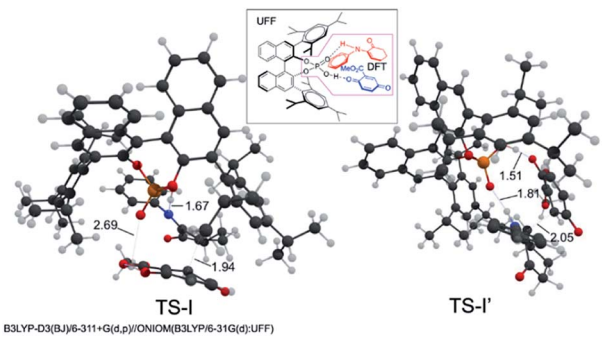

Fig. 4 Optimized geometries and the key bond lengths of TS-I and TS-I′ with CPA5.

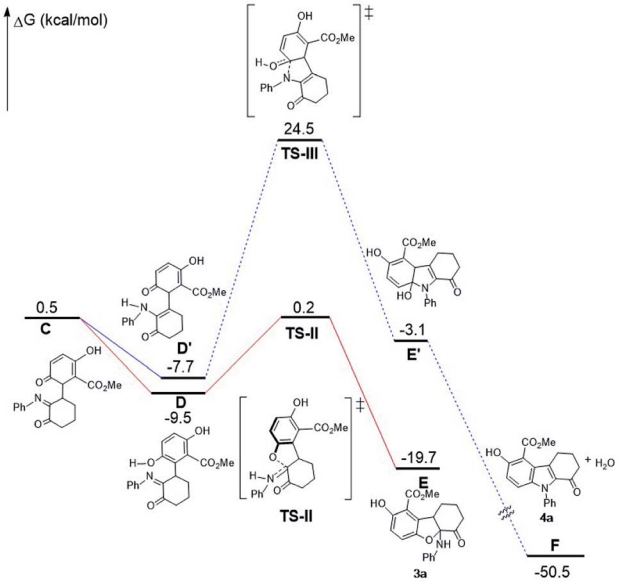

Fig. 5 Free-energy profiles calculated for the background reaction without catalyst.

Conclusions

The first example of a double divergent process has been developed for the reaction of α-enaminone with quinone ester. This double divergent process involves a catalyst (phosphoric acid)-controlled and an additive (molecular sieves)-controlled process. Facile manipulation of catalyst and additive leads to structurally completely different products. The roles of phosphoric acid and the molecular sieves were investigated through experiments and theoretical calculations. Our studies suggest that the phosphoric acid serves to lower the transition state energy and to promote amide formation leading to the formal aza-[3 + 2] cycloaddition to give the thermodynamic product. Our studies also show that M.S. do not play its traditional role as drying agent and/or H_2O mediator in the reactions. It was found that M.S. could affect the acidity of the phosphoric acid and serve to facilitate electron transfer in the process, disclosing a new role of molecular sieves. It is proposed that M.S. initiate a kinetic pathway to favor the formal oxo-[3 + 2] cycloaddition in the presence of phosphoric acid catalyst.

This work has introduced new reaction patterns, providing two novel formal oxo- and aza-[3 + 2] cycloaddition reactions. Both reactions are highly efficient, producing the corresponding 2,3-dihydrobenzofurans and *N*-substituted indoles in good yields with wide substrate scopes. The formal oxo-[3 + 2] cycloaddition reaction is highly stereoselectivity with up to >95 : 5 d.r. and 99% ee. Theoretical calculations conducted for enantio-determining TSs support the experimental data.

This work has also revealed a new set of reactivity of rarely explored α-enaminones. The α-enaminones displayed multifunctionality serving as both an enamine and a nitrogen nucleophile, and an imine electrophile in the divergent reaction. This divergent reaction offers new concise routes to access

enantioenriched 2,3-dihydrobenzofurans and *N*-substituted indoles, both of which are of biological and synthetic importance. Investigation of new reactions of α-enaminones are underway in our laboratory.

Conflicts of interest

There are no conflicts to declare.

Acknowledgements

We acknowledge the National Science Foundation MRI Program (CHE-1726652) and the University of North Texas for supporting the acquisition of the Rigaku XtaLAB Synergy-S X-ray diffractometer. Z. S. and T. R. C. thank the NSF for their support of this work *via* grants CHE-1464943 and CHE-1531468, the latter funding the purchase of the UNT Dept. of Chemistry high-performance computing cluster. We thank Dr Guido Verbeck and the Laboratory for Imaging Mass Spectrometry at the University of North Texas for Mass Spectrometry data. W. L. is grateful for University of North Texas for providing financial support.

Notes and references

1 For selected reviews, see: (*a*) J. Mahatthananchai, A. M. Dumas and J. W. Bode, *Angew. Chem., Int. Ed.*, 2012, **51**, 10954; (*b*) G. Zhan, W. Du and Y.-C. Chen, *Chem. Soc. Rev.*, 2017, **46**, 1675; (*c*) Y.-C. Lee, K. Kumar and H. Waldmann, *Angew. Chem., Int. Ed.*, 2018, **57**, 5212.

2 For selected examples, see: (*a*) S. Brandau, E. Maerten and K. A. Jørgensen, *J. Am. Chem. Soc.*, 2006, **128**, 14986; (*b*) Y. Zhu, X. H. Chen, M. S. Xie, S. X. Dong, Z. Qiao, L. L. Lin, X. H. Liu and X. M. Feng, *Chem.–Eur. J.*, 2010, **16**, 11963; (*c*) H. Shang, Y. Wang, Y. Tian, J. Feng and Y. Tang, *Angew. Chem., Int. Ed.*, 2014, **53**, 5662; (*d*) J.-Y. Liao, P.-L. Shao and Y. Zhao, *J. Am. Chem. Soc.*, 2015, **137**, 628; (*e*) W. Du, Q. Gu, Z. Li and D. Yang, *J. Am. Chem. Soc.*, 2015, **137**, 1130; (*f*) H. V. Adcock, E. Chatzopoulou and P. W. Davies, *Angew. Chem., Int. Ed.*, 2015, **54**, 15525; (*g*) L. Næsborg, K. S. Halskov, F. Tur, S. M. N. Mønsted and K. A. Jørgensen, *Angew. Chem., Int. Ed.*, 2015, **54**, 10193; (*h*) T. Hashimoto, H. Nakatsu and K. Maruoka, *Angew. Chem., Int. Ed.*, 2015, **54**, 4617; (*i*) G. Zhan, M.-L. Shi, Q. He, W.-J. Lin, Q. Ouyang, W. Du and Y.-C. Chen, *Angew. Chem., Int. Ed.*, 2016, **55**, 2147; (*j*) J.-J. Feng, T.-Y. Lin, C.-Z. Zhu, H. Wang, H.-H. Wu and J. Zhang, *J. Am. Chem. Soc.*, 2016, **138**, 2178; (*k*) Q.-Q. Cheng, J. Yedoyan, H. Arman and M. P. Doyle, *J. Am. Chem. Soc.*, 2016, **138**, 44; (*l*) Q.-Q. Cheng, M. Lankelma, D. Wherritt, H. Arman and M. P. Doyle, *J. Am. Chem. Soc.*, 2017, **139**, 9839; (*m*) L. Wang, S. Li, M. Blgmel, R. Puttreddy, A. Peuronen, K. Rissanen and D. Enders, *Angew. Chem., Int. Ed.*, 2017, **56**, 8516; (*n*) Y. Deng, L. A. Massey, Y. A. Rodriguez Núñez, H. Arman and M. P. Doyle, *Angew. Chem., Int. Ed.*, 2017, **56**, 12292; (*o*) Z. Liu, P. Sivaguru, G. Zanoni, E. A. Anderson and X. Bi, *Angew. Chem., Int. Ed.*, 2018, **57**, 8927; (*p*) H.-K. Liu, S. R. Wang, X.-Y. Song, L.-P. Zhao, L. Wang and Y. Tang, *Angew. Chem., Int. Ed.*, 2019, **58**, 4345; (*q*) S. Wei, L. Yin, S. R. Wang and Y. Tang, *Org. Lett.*, 2019, **21**, 1458.

3 (*a*) H.-J. Knölker and K. R. Reddy, *Chem. Rev.*, 2002, **102**, 4303; (*b*) G. R. Humphrey and J. T. Kuethe, *Chem. Rev.*, 2006, **106**, 2875; (*c*) A. J. Kochanowska-Karamyan and M. T. Hamann, *Chem. Rev.*, 2010, **110**, 4489; (*d*) N. Chida, *Top. Curr. Chem.*, 2011, **299**, 1; (*e*) S. Müller, M. J. Webber and B. List, *J. Am. Chem. Soc.*, 2011, **133**, 18534; (*f*) A. W. Schmidt, K. R. Reddy and H.-J. Knölker, *Chem. Rev.*, 2012, **112**, 3193; (*g*) H. Khanam and Shamsuzzaman, *Eur. J. Med. Chem.*, 2015, **97**, 483; (*h*) Q. Tian, J. Bai, B. Chen and G. Zhang, *Org. Lett.*, 2016, **18**, 1828; (*i*) R. Li and G. Dong, *Angew. Chem., Int. Ed.*, 2018, **57**, 1697; (*j*) N. Hu, H. Jung, Y. Zheng, J. Lee, L. Zhang, Z. Ullah, X. Xie, K. Harms, M. H. Baik and E. Meggers, *Angew. Chem., Int. Ed.*, 2018, **57**, 6242; (*k*) F. Tan and H.-G. Cheng, *Chem. Commun.*, 2019, **55**, 6151; (*l*) D. A. Vargas, R. L. Khade, Y. Zhang and R. Fasan, *Angew. Chem., Int. Ed.*, 2019, **58**, 10148; (*m*) Q. Zhang, F.-M. Zhang, C.-S. Zhang, S.-Z. Liu, J.-M. Tian, S.-H. Wang, X.-M. Zhang and Y.-Q. Tu, *Nat. Commun.*, 2019, **10**, 2507; (*n*) R. P. Pandit, S. T. Kim and D. H. Ryu, *Angew. Chem., Int. Ed.*, 2019, **58**, 13427; (*o*) Q. Zhao, J.-K. Jin, J. Wang, F.-L. Zhang and Y.-F. Wang, *Chem. Sci.*, 2020, **11**, 3909; (*p*) S. J. O'Malley, K. L. Tan, A. Watzke, R. G. Bergman and J. A. Ellman, *J. Am. Chem. Soc.*, 2005, **127**, 13496; (*q*) J. Alemán, S. Cabrera, E. Maerten, J. Overgaard and K. A. Jørgensen, *Angew. Chem., Int. Ed.*, 2007, **46**, 5520; (*r*) C. Gelis, M. Bekkaye, C. Lebée, F. Blanchard and G. Masson, *Org. Lett.*, 2016, **18**, 3422; (*s*) L. Liao, C. Shu, M. Zhang, Y. Liao, X. Hu, Y. Zhang, Z. Wu, W. Yuan and X. Zhang, *Angew. Chem., Int. Ed.*, 2014, **53**, 10471; (*t*) L. Zhang, J. Hu, R. Xu, S. Pan, X. Zeng and G. Zhong, *Adv. Synth. Catal.*, 2019, **361**, 5449; (*u*) Q. Yu, Y. Fu, J. Huang, J. Qin, H. Zuo, Y. Wu and F. Zhong, *ACS Catal.*, 2019, **9**, 7285; (*v*) W. Feng, H. Yang, Z. Wang, B.-B. Gou, J. Chen and L. Zhou, *Org. Lett.*, 2018, **20**, 2929.

4 (*a*) J. V. Greenhill, *Chem. Soc. Rev.*, 1977, **6**, 277; (*b*) A.-Z. A. Elassar and A. A. El-Khair, *Tetrahedron*, 2003, **59**, 8463; (*c*) H. Seki and G. I. Georg, *J. Am. Chem. Soc.*, 2010, **132**, 15512; (*d*) A. Palmieri, S. Gabrielli, C. Cimarelli and R. Ballini, *Green Chem.*, 2011, **13**, 3333; (*e*) D. Yu, Y. N. Sum, A. C. C. Ean, M. P. Chin and Y. Zhang, *Angew. Chem., Int. Ed.*, 2013, **52**, 5125; (*f*) Y.-W. Kang, Y. J. Cho, S. J. Han and H.-Y. Jang, *Org. Lett.*, 2016, **18**, 272; (*g*) S. Arshadi, E. Vessally, L. Edjlali, E. Ghorbani-Kalhor and R. Hosseinzadeh-Khanmiri, *RSC Adv.*, 2017, **7**, 13198; (*h*) G. Fang, J. Liu, J. Fu, Q. Liu and X. Bi, *Org. Lett.*, 2017, **19**, 1346; (*i*) Z. Dong, X. W. Zhang, W. Li, Z. M. Li, W. Y. Wang, Y. Zhang, W. Liu and W. B. Liu, *Org. Lett.*, 2019, **21**, 1082.

5 (*a*) M. Rueping and A. Parra, *Org. Lett.*, 2010, **12**, 5281; (*b*) Y.-J. Li, L. Zhang, N. Yan, X.-H. Meng and Y.-L. Zhao, *Adv. Synth. Catal.*, 2018, **360**, 455; (*c*) K. Hu, P. Qian, J. Su, Z. Li, J. Wang, Z. Zha and Z. Wang, *J. Org. Chem.*, 2019, **84**, 1647; (*d*) B. Xu, Y. Shang, X. Jie, X. Zhang, J. Kan, S. L. Yedagea and W. Su, *Green Chem.*, 2020, **22**, 1827; (*e*)

E. H. N. Fernando, J. Cortes Vazquez, W. Luo, V. N. Nesterov and H. Wang, unpublished results.

6 (*a*) Z. Xu, L. Liu, K. Wheeler and H. Wang, *Angew. Chem., Int. Ed.*, 2011, **50**, 3484; (*b*) Y. Deng, L. Liu, R. G. Sarkisian, K. Wheeler, H. Wang and Z. Xu, *Angew. Chem., Int. Ed.*, 2013, **52**, 3663; (*c*) Y. Deng, S. Kumar and H. Wang, *Chem. Commun.*, 2014, **50**, 4272; (*d*) Y. Deng, S. Kumar, K. Wheeler and H. Wang, *Chem.–Eur. J.*, 2015, **21**, 7874; (*e*) Y. Deng, C. V. Karunaratne, E. Csatary, D. L. Tierney, K. Wheeler and H. Wang, *J. Org. Chem.*, 2015, **80**, 7984; (*f*) C. V. Karunaratne, R. G. Sarkisian, J. Reeves, Y. Deng, K. A. Wheeler and H. Wang, *Org. Biomol. Chem.*, 2017, **15**, 4933.

7 (*a*) C. Paal, *Ber. Dtsch. Chem. Ges.*, 1884, **17**, 2756; (*b*) L. Knorr, *Ber. Dtsch. Chem. Ges.*, 1884, **17**, 2863; (*c*) V. Amarnath, D. C. Anthony, K. Amarnath, W. M. Valentine, L. A. Wetterau and D. G. Graham, *J. Org. Chem.*, 1991, **56**, 6924; (*d*) V. Amarnath and K. Amamath, *J. Org. Chem.*, 1995, **60**, 301; (*e*) G. Yin, Z. Wang, A. Chen, M. Gao, A. Wu and Y. Pan, *J. Org. Chem.*, 2008, **73**, 3377; (*f*) L. Zhang, J. Zhang, J. Ma, D.-J. Cheng and B. Tan, *J. Am. Chem. Soc.*, 2017, **139**, 1714.

8 (*a*) D. A. Evans and J. Wu, *J. Am. Chem. Soc.*, 2003, **125**, 10162; (*b*) Y.-H. Chen, D.-J. Cheng, J. Zhang, Y. Wang, X.-Y. Liu and B. Tan, *J. Am. Chem. Soc.*, 2015, **137**, 15062; (*c*) H. F. Zheng, C. R. Xu, Y. Wang, T. F. Kang, X. H. Liu, L. L. Lin and X. M. Feng, *Chem. Commun.*, 2017, **53**, 6585; (*d*) C. R. Xu, H. F. Zheng, B. W. Hu, X. H. Liu, L. L. Lin and X. M. Feng, *Chem. Commun.*, 2017, **53**, 9741; (*e*) Q.-J. Liu, J. Zhu, X.-Y. Song, L. Wang, S. R. Wang and Y. Tang, *Angew. Chem., Int. Ed.*, 2018, **57**, 3810; (*f*) X. Zhang, Y.-H. Chen and B. Tan, *Tetrahedron Lett.*, 2018, **59**, 473; (*g*) D.-L. Lu, Y.-H. Chen, S.-H. Xiang, P. Yu, B. Tan and S. Li, *Org. Lett.*, 2019, **21**, 6000; (*h*) G. Coombs, M. H. Sak and S. J. Miller, *Angew. Chem., Int. Ed.*, 2020, **59**, 2875.

9 (*a*) D. Parmar, E. Sugiono, S. Raja and M. Rueping, *Chem. Rev.*, 2014, **114**, 9047; (*b*) L. Hong, W. Sun, D. Yang, G. Li and R. Wang, *Chem. Rev.*, 2016, **116**, 4006.

10 CCDC 1919282 (**3a**), 1921254 (**3w**) and 1919286 (**4a**) contain the supplementary crystallographic data for this paper.

11 (*a*) S. L. Li, C. Yang, Q. Wu, H. L. Zheng, X. Li and J. P. Cheng, *J. Am. Chem. Soc.*, 2018, **140**, 12836; (*b*) Y. B. Wang and B. Tan, *Acc. Chem. Res.*, 2018, **51**, 534; (*c*) X. Fan, X. Zhang, C. Li and Z. Gu, *ACS Catal.*, 2019, **9**, 2286; (*d*) Y. Kwon, J. Li, J. P. Reid, J. M. Crawford, R. Jacob, M. S. Sigman, F. D. Toste and S. J. Miller, *J. Am. Chem. Soc.*, 2019, **141**, 6698; (*e*) H. Li, X. Yan, J. Zhang, W. Guo, J. Jiang and J. Wang, *Angew. Chem., Int. Ed.*, 2019, **58**, 6732; (*f*) L. Zhang, S. H. Xiang, J. J. Wang, J. Xiao, J. Q. Wang and B. Tan, *Nat. Commun.*, 2019, **10**, 566; (*g*) W. Xia, Q.-J. An, S.-H. Xiang, S. Li, Y.-B. Wang and B. Tan, *Angew. Chem., Int. Ed.*, 2020, **59**, 6775.

12 (*a*) L. Chang, Y. L. Kuang, B. Qin, X. Zhou, X. H. Liu, L. L. Lin and X. M. Feng, *Org. Lett.*, 2010, **12**, 2214; (*b*) W. Yang, Z. Wang and J. Sun, *Angew. Chem., Int. Ed.*, 2016, **55**, 6954; (*c*) W. W. Luo, Z. C. Sun, E. H. N. Fernando, V. N. Nesterov, T. R. Cundari and H. Wang, *ACS Catal.*, 2019, **9**, 8285.